Chromatographic retention behaviour, modelling and optimization of a UHPLC-UV separation of the regioisomers of the Novel Psychoactive Substance (NPS) methoxphenidine (MXP)

Bernard O. Boateng[a], Mark Fever[b], Darren Edwards[a,d], Patrik Petersson[c], Melvin R. Euerby[a,b,e,*] and Oliver B. Sutcliffe[f,*]

[a] Strathclyde Institute of Pharmacy and Biomedical Sciences, University of Strathclyde, 161 Cathedral Street, Glasgow, G4 0RE, UK.

[b] Hichrom Ltd, 1 The Markham Centre, Station Road, Theale, Reading Berkshire, RG7 4PE, UK.

[c] Novo Nordisk A/S, Novo Nordisk Park, DK-2760 Måløv, Denmark.

[d] Present address: Drug Discovery Unit, School of Life Sciences, Sir James Black Centre, University of Dundee, Dow Street, Dundee DD1 5EH, Scotland, UK.

[e] Present address: Shimadzu UK Limited, Mill Court, Featherstone Road, Wolverton Mill South, Milton Keynes, MK12 5RD, UK.

[f] MANchester DRug Analysis and Knowledge Exchange (MANDRAKE), School of Science and the Environment, Faculty of Science and Engineering, Manchester Metropolitan University, John Dalton Building, Chester Street, Manchester, M1 5GD, UK.

* corresponding authors, melvin.euerby@strath.ac.uk and o.sutcliffe@mmu.ac.uk

Abstract

A detailed investigation into the chromatographic retention behaviour and separation of the three regioisomers of the Novel Psychoactive Substance (NPS) methoxphenidine (i.e. 2-, 3- and 4-MXP isomers) has revealed the ionization state of the analyte and stationary phase, to be the controlling factor in dictating which retention mechanism is in operation. At low pH, poor separation and retention was observed. In contrast, at intermediate pH, enhanced retention and separation of the three MXP isomers was obtained; it appeared that there was a synergistic effect between the electrostatic and hydrophobic mechanisms. At high pH, the MXP isomers were retained by hydrophobic retention. Accurate retention time predictions (<0.5%) were achievable using non-linear retention models (3 x 3). This allowed the optimization of the gradient separation of the MXP isomers using a two-dimensional gradient and temperature design space. Prediction errors for peak width and resolution were, in most cases, lower than 5%. The use of linear models (2 x 2) still afforded retention time and resolution accuracies of < 2.3 and 11% respectively. A rapid and highly sensitive LC-MS friendly method (i.e. $R_{s\ min} > 3$ within 2.5 minutes) was predicted and verified. The

developed methodology should be highly suitable for the rapid, specific and sensitive detection and control of MXP regioisomers.

Keywords

- Reversed phase HPLC
- Two-dimensional retention modelling
- Regioisomeric methoxyphenidines
- Novel Psychoactive Substance
- Chromatographic optimization
- Retention mechanisms

1 Introduction

Designer drugs are analogues of controlled substances that are designed to produce effects similar to the controlled substances they mimic" [1]. The rate at which such substances are appearing poses significant issues for forensic laboratories with respect to identification and quantification, as validated analytical methods and reference standards are not usually available [4].

Dissociative diarylethylamine anaesthetics (Figure 1) such as diphenidine (1) [5] and 2-methoxphenidine (2-MXP, 2) [6] are substances that distort perceptions, produce feelings of detachment and induce a state of anaesthesia by antagonising ionotropic *N*-methyl-*D*-aspartate receptors (NMDAR) in the central nervous system [7]. Though both the supply and production of diphenidine and 2-methoxphenidine is now controlled in the United Kingdom by the Psychoactive Substances Act (2016) [8], the global prevalence of novel diarylethylamine derivatives still raises considerable legal and analytical challenges in the forensic identification of these materials. 2-MXP has been implicated in a number of fatalities in Europe [9, 10] and is encountered in both tablet and powder forms. Recently, the reversed-phase liquid chromatographic (RP-LC) separation of the regioisomers of methoxphenidine (2-MXP, 2; 3-MXP, 3 and 4-MXP, 4, see Figure 1) has been reported using a superficially porous phenyl hexyl material (i.e. 2.6 µm Kinetex) coupled with a shallow MeCN / formic acid gradient at 30 °C (i.e. 0.25% MeCN/min). While the 2-isomer was well resolved from the other two isomers, only partial separation of the 3- and 4-isomers was observed (the elution order was reported to be 3-MXP, 4-MXP, 2-MXP isomer). However, the paper [6] did not prove evidence of any systematic investigation into the retention behaviour. Analytical differentiation of regioisomers is a significant issue in forensic drug analysis, because, in most cases, legal controls are placed on only one or two of the conceivable isomers and require a forensic scientist to show unequivocally that a sample submitted is in fact a controlled drug and not one of the non-controlled regioisomers. This can be readily achieved using Nuclear Magnetic Resonance (NMR) spectroscopy, however, few forensic laboratories have such instruments and the discrimination of regioisomers using the technique is both cost and labour intensive. Geyer *et al.* has recently published a

validated GC-(EI)-MS protocol for the qualitative and quantitative analysis of thirteen diarylethylamine derivatives (including 2-MXP and its isomers) in seized powder samples – however, the published method has significant limitations in terms of overall analysis time (*circa.* 45 mins) [11]. This HPLC method provides, for the first time, both a general screening method and quantification of the active components for seized solid samples of methoxphenidine, which is significantly superior to the previously reported GC-MS [11] and HPLC [6, 10] methods in terms of overall run time (7 mins) and resolution of the regioisomers.

In contrast, this current paper reports the retention behaviour and separation of the three regioisomeric methoxphenidines as a function of pH, temperature, proportion of organic modifier and buffer concentration on a variety of RP columns of widely differing chromatographic selectivity. Six new generation RP silica phases were selected from the same manufacturer in order to minimize any problems associated with differing base silica acidities [12]. Three totally porous particles (TPP) (i.e. C18-AR, C18 and C18-PFP) were selected as previously these stationary phases have demonstrated complementary chromatographic selectivity to each other [12]. In addition, three high pH stable phases (which have been shown to possess similar selectivity to their non-high pH stable TPP counterparts [i.e. TPP C18 versus the TPP and superficially porous particles (SPP) SuperC18 materials plus the TPP C18-AR and SPP Super Phenyl hexyl phases] were additionally selected in order to allow the basic MXP regioisomers to be chromatographed, at high pH, in their ion-suppressed form. The three-high pH stable phases have been reported to show good stability up to pH 11 [13].

A detailed investigation into the retention mechanism of these regioisomeric substances was performed as a function of stationary phase chemistry, mobile phase pH, proportion of organic modifier and buffer concentration. The most promising chromatographic conditions were then subjected to retention modelling and optimization in order to develop a rapid, highly selective and robust UHPLC-UV separation of the 2-, 3- and 4-MXP isomers, within bulk forensic samples, using LC-MS friendly conditions.

2 Materials and methods

2.1 Chemicals and Reagents

All water and solvents used were HPLC grade, test analytes and mobile phase chemicals were supplied by Sigma-Aldrich (Poole, UK) and Fisher Scientific (Loughborough, UK). Samples of the three methoxphenidine isomers (2 – 4) were prepared, under UK [Home Office] Drug Licence (No. 337201), as their corresponding hydrochloride salts at Manchester Metropolitan University. The synthesis of the racemic target compounds was achieved using the previously reported method [11] in 52 – 77% overall yield. The hydrochloride salts were obtained as stable, colourless to off-white powders (Figure 1) and determined to be soluble (10 mg mL^{-1}) in deionised water, methanol, dichloromethane and dimethylsulfoxide. To ensure the authenticity of the materials utilized in this study the three synthesized samples

were fully structurally characterized by ^{1}H-NMR, ^{13}C-NMR, GC-MS and ATR-FTIR and the purity of all samples confirmed by elemental analysis (>99.5% in all cases) [11].

2.1.1 Methoxphenidine (MXP) isomers

Stock solutions of the individual isomers of methoxphenidine were made up in MeCN/water (1:1 v/v) at a concentration of 1 mg mL^{-1}. A mixture of the isomers was prepared and then diluted to 100 µg mL^{-1} (of each isomer) with MeCN/water (1:1 v/v) for the chromatographic studies.

2.2 Software

LogD and pK_a values were predicted (ACD/Percepta, Toronto, Canada, version 2016.1.1) and retention modelling and optimization (ACD/LC Simulator, version 2016.1.1) were performed using software from ACD/Labs (Advanced Chemistry Development Inc., Toronto, Canada). Buffers of a desired pH and buffer concentration were determined by the Buffer Maker software (ChemBuddy, Marki, Poland, version 1.0.1.55).

2.3 Instrumentation

2.3.1 UHPLC instrumentation

UHPLC was performed on the following instrumentation: Agilent 1290 Infinity UHPLC systems (Agilent Technologies, Waldbronn, Germany) equipped with either binary (model G4220A) or quaternary (model G4204A) pumps used in conjunction with an integrated degasser (model G4220A), autosampler (model G4226A), column oven model (G1316C), photodiode array detector (model G4212A) equipped with a 1 µL / 10 mm pathlength flow cell, 380 µL Jet Weaver mixer and a 12 position / 13 port solvent selection valve (model G1160A), was used to allow the automated selection of up to 12 different eluents from mobile phase line C of the Agilent 1290 Infinity quaternary UHPLC, the system(s) was controlled and data collected by means of ChemStation (Agilent Technologies, Waldbronn, Germany, version B.04.03). Shimadzu Nexera X2 UHPLC (Shimadzu UK Ltd, Milton Keynes, UK) equipped with LC-30AD pumps, DGU-20A5R degassers, SIL-30AC autosampler, CTO-20AC column oven, SPD-M30A photodiode array detector equipped with a 10 µL / 10 mm pathlength flow cell, 180 µL mixer, the system was controlled and data collected by means of LabSolutions software (Shimadzu UK Ltd, Milton Keynes, UK, version 5.86).

2.4 Liquid Chromatography

pH measurements were recorded in the aqueous fraction of the mobile phase and quoted as $^{w}{}_{w}$pH. At least 20 column volumes of the appropriate mobile phase were flushed through the columns prior to commencing the testing or on changing the mobile phase

conditions. The totally porous ACE C18, C18-PFP, C18-AR (5 µm, 100Å, 150 x 4.6 mm I.D. format), C18-AR, SuperC18 (3 µm, 100Å, 50 x 4.6 mm I.D. format), ACE UltraCore superficially porous SuperC18 and SuperPhenylhexyl (2.5 µm, 100Å, 50 x 4.6 mm I.D. format) columns were as supplied by Advanced Chromatography Technologies (Aberdeen, Scotland, UK). The integrity of all the columns was confirmed periodically throughout the experiments by injecting a suitable non-polar test mixture (i.e. uracil, toluene, biphenyl, dimethyl phthlate and phenanthrene) before and after the experiments. All columns gave retention times, efficiency and peak symmetry levels >95% of their initial value. The mobile phase was degassed and mixed on-line for the aqueous / organic mixtures.

The first baseline disturbance for a water injection was used as the dead time (t_M) marker. A flow rate of 1.0 mL min^{-1} and a 2 µL injection was used in all experiments and a column temperature was maintained between 20 – 70 °C. The diode array detector was set to monitor a wavelength of 278 nm with a reference at 360 nm. The data sampling rate was set at 40 Hz. Peak width and symmetry was determined at half height as reported by the ChemStation software or LabSolutions software. For the retention modelling the peak width at base was calculated by multiplying the peak width at half height by 1.699 [to generate the 4σ, United States Pharmacopeia (USP) peak width values]. Chromatographic values reported are the average of duplicate injections. Retention factors (k) were calculated for isocratic conditions using the following equation; $k = (t_R – t_M)/ t_M$. Where t_R = retention time of the isomer and t_M = void time of an unretained analyte.

2.4.1 Effect of ammonium acetate concentration on the retention of the MXP isomers (see section 3.3)

Evaluation of the effect of ammonium acetate (pH 6.8) concentration (1 – 14 mM) on the retention of the methoxphenidine isomers was performed on an ACE C18-AR 3 µm 50 x 4.6 mm column at 54 % MeCN concentration, 30 °C, 1 mL min^{-1} using the Agilent 1290 Infinity Quaternary UHPLC. Mobile phase A) 100 mM ammonium acetate (pH 6.8 unadjusted), B) MeCN, C) water. The appropriate buffer concentrates were mixed on-line, for example 10 mM buffer in MeCN/water was prepared by mixing A:B:C in the ratio 10:54:36 v/v/v.

2.4.2 Effect of the proportion of acetonitrile (MeCN) on the retention of the MXP isomers (see section 3.4)

Evaluation of the effect of the proportion of MeCN (18 – 63 % v/v) on the retention of the methoxphenidine isomers was performed on an ACE C18-AR and ACE SuperC18, 3 µm, 50 x 4.6 mm column, 1 mL min^{-1}, 60 °C, mobile phase A) 10 mM ammonium acetate (pH 6.8 unadjusted), 10 mM ammonium formate (pH 3) or 18.6 mM ammonia (pH 10.7) in water, B) the appropriate buffer in MeCN/water (9:1 v/v) using the Agilent 1290 Infinity Binary UHPLC.

2.4.3 Effect of temperature on the retention of the MXP isomers (see section 3.5)

Evaluation of the effect of temperature (20 -70 °C) on the retention of the methoxphenidine isomers was performed on an ACE C18-AR, 3 µm, 50 x 4.6 mm column using 60 %B (i.e. 54 % v/v MeCN), 1 mL min^{-1}, mobile phase A) 10 mM ammonium acetate (pH 6.8 unadjusted) in water, B) 10 mM ammonium acetate (pH of 6.8 unadjusted) in MeCN/water (9:1 v/v) using the Shimadzu Nexera X2 UHPLC.

2.4.4 Effect of pH on the retention of the MXP isomers (see section 3.2)

Evaluation of the effect of pH on the retention of the methoxphenidine isomers was performed on ACE UltraCore SuperC18 and C18-AR columns, 2.5 and 3 µm respectively, 50 x 4.6 mm column at 60 %B (i.e. 54 % v/v MeCN), 50 °C, 1 mL min^{-1}, mobile phase A) 10 mM ammonium formate pH 3, B) 10 mM ammonium acetate (unadjusted pH of 6.8) and c) 18 mM ammonia (unadjusted pH of 10.7) using the Agilent 1290 Infinity Quaternary UHPLC.

2.4.5 Effect of pH over the range pH 8 -10.7 on the retention of the MXP isomers (see section 3.2.3)

Evaluation of the effect of high pH (pH 8, 9, 9.25, 9.5, 9.75, 10 and 10.7) on the retention of the methoxphenidine isomers was performed on an ACE Ultracore SuperC18, 2.5 µm, 50 x 4.6 mm column using 10 mM ammonia / acetic acid buffers (ammonia concentration kept constant) in MeCN/water (54:46 v/v), 50 °C, 1 mL min^{-1} using the Agilent 1290 Infinity Quaternary UHPLC. Stock pH buffers were prepared as described by the Buffer Maker Software.

2.5 Retention modelling

2.5.1 Two-dimensional retention modelling and optimization: Gradient time *versus* temperature on the C18-AR at pH 6.8 (see section 3.7.2)

An ACE C18-AR column (3 µm, 50 x 4.6 mm) was used at a flow rate of 1 mL min^{-1} using the Shimadzu Nexera X2 UHPLC. Sixteen input runs and six validation runs were performed (see section 3.7.2, Figure 6). Mobile phase A consisted of 10 mM ammonium acetate (unadjusted pH 6.8) and mobile phase B of 10 mM ammonium acetate (unadjusted pH 6.8) in MeCN/water (9:1 v/v). A temperature range of 30 to 70 °C was investigated (see Figure 6). The %B gradient range was run between 40 and 70 %B. After the selected gradient run time (t_G) was reached, a 5-minute hold time at 70%B, 1-minute ramp down to 40%B, and a 5-minute post time at 40%B were employed.

3 Results and Discussion

3.1 Chromatographic separation of the methoxphenidine (MXP) regioisomers as a function of stationary phase chemistry

The TPP ACE C18, C18-AR and C18-PFP and the high pH stable SPP SuperC18 and SuperPhenylhexyl phases, which possess differing bonded ligands on the silica, have recently been showed to exhibit differing chromatographic selectivities (see Supplementary electronic information Table SEI 1) due to the ligands' differing propensity to participate in hydrophobic, aromatic (i.e. π acid and π base interactions), dipole – dipole interactions, hydrogen bonding and electrostatic interaction with various analytes under a range of chromatographic conditions [13]. Hence, it was somewhat surprising that these phases failed to exhibit any major selectivity differences irrespective of mobile phase pH suggesting that the MXP interactions with the differing stationary phase ligands was not the controlling retention mechanism.

3.2 Chromatographic separation of the methoxphenidine (MXP) regioi-somers as a function of pH

The regioisomers of methoxphenidine are hydrophobic compounds with tertiary amine functionality, with calculated pK_a values of 8.7, 9.1 and 9.4 for the 2-, 3- and 4-MXP isomers respectively. Hence, the effect of pH was investigated in order to assess the influence of hydrophobic and electrostatic interactions on their chromatographic retention.

3.2.1 Chromatographic separation of the methoxphenidine (MXP) regioisomers at low pH

Chromatography of the regioisomeric analytes (Figure 1, 2 – 4) on the TPP ACE C18, C18-AR and C18-PFP, at low pH, resulted in low retention and only partial separation of the isomers (data not shown). The low retention and the elution order observed on the three TPP phases, at low pH with 10 mM ammonium formate pH 3 mirrored that was previously reported by McLaughlin *et al* [6] using another phenylhexyl phase (i.e. the 2-isomer (2) eluted after the partial separation of the 3- and 4- isomers). Separation selectivity was not improved even when lower %MeCN containing mobile phases were employed in order to improve retention (see Figure 4a). The low retention (see Figure 2a for a typical chromatogram on the SPP SuperC18 column) may be attributed to the mutual repulsion of the adsorbed protonated MXP isomers and the low acidity of the new generation silica columns used in this study.

3.2.2 Chromatographic separation of the methoxphenidine (MXP) regioisomers at intermediate pH

Chromatography at pH 6.8 (i.e. 10 mM ammonia acetate) using the C18-AR, SuperC18 and SuperPhenylHexyl phases resulted in enhanced retention and excellent separation of the regioisomers (the C18 and C18-PFP phases were not evaluated). Figure 2b is typical of the separation that could be achieved on these phases at intermediate pH using the SPP SuperC18. Once again, the same elution order (i.e. 2-MXP, 4-MXP, 3-MXP) was obtained on each phase, which was surprising, given the large chromatographic selectivity differences that exists between the C18 and phenyl phases (see Supplementary electronic information Table SEI 1). The elution order at low and intermediate pH (i.e. 2-MXP, 4-MXP, 3-MXP) was different to that observed at high pH (i.e. 4-MXP, 3-MXP, 2-MXP *see Figures 2a -c*).

3.2.3 Chromatographic separation of the methoxphenidine (MXP) regioisomers at high pH

Chromatography on the high pH stable SPP & TPP phases (i.e. SuperC18 and SuperPhenylHexyl) at pH 10.7 (i.e. 18 mM ammonia) exhibited enhanced retention and good resolution of all of the isomers with the same elution order (i.e. 4-MXP, 3-MXP, 2-MXP) irrespective of the phase chemistry. Figure 2c highlights a typical separation at high pH conditions using the SPP SuperC18 phase. Interestingly, the elution order of the isomers at high pH was different to that observed using intermediate pH conditions (i.e. 2-MXP, 4-MXP, 3-MXP). It is presumed that the high pH of the mobile phase renders the MXP molecules uncharged hence eliminating the possibility of ion exchange interactions and increasing the hydrophobic and π-π interaction of the neutral MXP analytes with the stationary phase. As only small differences in selectivity were observed between the C18 and phenyl phases, we must conclude that there is minimal π-π interaction of the analytes with the phenyl phase, this may be attributed to the fact that MeCN was used as the organic modifier [14,15].

The retention of each of the isomers was in line with their estimated logD values in that greater retention was observed at pH 10.7 when the MXP isomers were in their unionized forms. (e.g. the 4-MXP's LogD values were estimated at pH 3, 6.8 and 10.7 to be 1.76, 2.41 and 4.84 respectively).

In order to gain a better understanding of the retention behaviour of the MXP isomers at pH conditions spanning their estimated pK_a values [i.e. ACD Percepta estimates of 9.4 (4-MXP), 9.1 (3-MXP), and 8.7 (2-MXP)] their retention over the pH range of 8 – 11 was investigated on the high pH stable SPP SuperC18 at constant ammonia concentration (see Supplementary electronic information Figure SEI 1). Up to a $^{w}{}_{w}$pH of 9.5, the elution order remained the same as that at pH 6.8; the retention of all the isomers becoming progressively longer presumably due to a greater influence from hydrophobic retention mechanisms as the mobile phases becomes progressively more alkaline and the MXP isomers less protonated. Between $^{w}{}_{w}$pH 9.75 and 11 (the latter is the maximum operating pH for this phase) a switch in the elution order was observed. The 2-MXP which between $^{w}{}_{w}$pH 6.8 – 9.5 eluted before the 4-MXP and 3-MXP isomers respectively, at $^{w}{}_{w}$pH 11 eluted after the 4-MXP and 3-MXP isomers respectively. The same observations were seen on

309 another high pH stable phase (i.e. the bridged ethyl hybrid - XBridge C18 phase – data not
310 shown).

311 Addition of sodium chloride into the high pH mobile phase with the TPP SuperC18 phase
312 (see Supplementary electronic information Figure SEI 2) failed to affect the retention time of
313 the MXP regioisomers due to the fact that they were chromatographed in their ion-
314 suppressed form at pH 10.7 (i.e. as the free bases). In comparison, the addition of sodium
315 chloride to the intermediate pH mobile decreased the retention of the methoxphenidine
316 isomer as expected due to competition of the positively charged sodium and MXP ions for
317 the negatively charged silanol groups on the surface of the stationary phase.

318 Due to the enhanced separation (i.e. resolution and speed) of the isomers at intermediate
319 pH, a more detailed study into the chromatographic parameters which control their
320 retention was performed at intermediate pH using the ACE C18-AR and SuperC18 phases as
321 phase chemistry did not appear to be a major factor in determining chromatographic
322 selectivity.

323

324 3.3 Effect of buffer concentration at intermediate pH

325 The effect of ammonium acetate concentration was investigated at 30 °C with a $^{w}{}_{w}$ pH 6.8
326 mobile phase on the C18-AR phase (see Figure 3). According to ion exchange theory [16-18]
327 retention has been proposed to be related to buffer concentration as expressed in Equation
328 1.

329

330 $\log k = a + b \log x$ Equation 1

331

332 where k = retention factor, a, b and c are coefficients and x = chromatographic variable (i.e.
333 proportion of organic or buffer concentration)

334

335 Equation 1 did not provide a good fit for the data shown in Figure 3 so a more complex
336 model, as described by Equation 2, was employed.

337

338 $\log k = a + b \log x + c (\log x)^2$ Equation 2

339

340 The observation that increased buffer concentrations generated reduced retention of the
341 MXP isomers highlighted that there is an ion exchange mechanism contributing to retention
342 at intermediate pH.

343
344

3.4 Effect of the proportion of MeCN at intermediate pH

In contrast to the expected linear relationship (see Equation 3) between the log *k* of the MXP isomers and the proportion of MeCN in the mobile phase [19, 20], a curved relationship (see Equation 4) was observed between the retention of the MXP isomers and the proportion of MeCN in the mobile phase at pH 6.8 (see Figure 4a for a typical example on the SuperC18 phase). The use of the standard second order polynomial model (see Equation 4) used in the retention modelling software was found to generate highly accurate retention predictions (see retention modelling sections 3.7.1 and 3.7.2).

$$\log k = a + b\,x \qquad \text{Equation 3}$$

$$\log k = a + b\,x + c\,x^2 \qquad \text{Equation 4}$$

The curved relationship suggested that, at intermediate pH, a mixed mode retention mechanism was in operation. The negatively charged silanol groups on the phase may attract the positively charged analytes, via an electrostatic attraction, into the hydrophobic phase where it can interact with the bonded ligands. A curved relationship (i.e. second order polynomial model) was also observed at low pH possibly due to a secondary ionic repulsive interaction (see Figure 4b). In comparison the relationship at pH 10.7 was observed to be much more linear (see Figure 4c) due to the fact that the MXP isomers were chromatographed in their ion suppressed form and hence a simple hydrophobic retention mechanism dominated.

3.5 Effect of temperature at intermediate pH

If a simple hydrophobic retention mechanism was in operation at pH 6.8, then as the temperature was increased the retention time should decrease (i.e. van't Hoff relationship) as shown in Equation 5.

$$\log k = a + \frac{b}{T} \qquad \text{Equation 5}$$

Where T = temperature

However, if the retention is dependent on multiple interactions, then non-linear responses may be generated and Equation 6 should be more appropriate [18, 21, 22].

$$\log k = a + \frac{b}{T} + \frac{c}{T^2} \qquad \text{Equation 6}$$

As can be seen in Figure 5, the retention of each MXP isomer on the ACE C18-AR phase behaved differently as a function of temperature in 10 mM ammonium acetate (pH 6.8) MeCN/water (54:46 v/v). The 2-MXP isomer exhibited the expected reduction in retention as temperature increased whereas temperature had little effect on the retention of the 3-MXP and 4-MXP isomers. These observations may reflect differential changes in the pK_a of the MXP isomers and the silanol groups on the stationary phase surface and the pH of the organic / aqueous mobile phase as temperature is changed and hence the degree of electrostatic interaction of the regioisomers with the ionized silanol groups. Therefore, it was inferred that the mechanism controlling the retention and separation of the MXP regioisomers at pH 6.8 was attributed to an electrostatic interaction which facilitated hydrophobic interactions.

3.6 Retention behaviour conclusions

Stationary phase chemistry appears to have minimal influence on the chromatographic selectivity of the three MXP regioisomers at low, intermediate or high pH mobile phase conditions. At low pH mobile phase conditions, the analytes exhibited minimal retention as a result of mutual repulsion of the adsorbed positively charged analyte on the low acidity stationary phases. In comparison, at intermediate pH enhanced retention and separation of the regioisomers was observed. This was attributed to a synergistic effect of the electrostatic attraction between the ionized analyte and the silanol groups which attracts the charged analyte into the lipophilic stationary phase where hydrophobic interactions could take place. In comparison, at high pH the MXP analytes are chromatographed on the SPP and TPP SuperC18 or phenyl hexyl phases in their neutral form and hydrophobic interactions were the major retention mechanism.

3.7 Two-dimensional retention modelling and optimization

The chromatographic separation of the three isomers was greater at pH 6.8 than at either pH 3 or 10.7 (see Figures 2a -c). This was further confirmed in preliminary two-dimensional (gradient time versus temperature) retention modelling studies using the SPP Super phenylhexyl and C18 phases, as a function of gradient time (i.e. 5 and 15 minutes) and temperature (i.e. 30 to 65°C) at pH 3 (gradient range 4.5 - 45% MeCN), 6.8 (36 - 90% MeCN) and 10.7 (36 - 90% MeCN). Four experimental input runs were used to construct the 2 x 2 models using Equations 3 and 5 in the commercial retention modelling software (see Supplementary electronic information Figures SEI 3 and 4).

3.7.1 Selection of the most appropriate retention models

From the preliminary two-dimensional retention modelling the following operating parameters were chosen to perform more detailed one-dimensional modelling studies using the ACE C18-AR, which was observed to generate sharper MXP peaks, to confirm which equations would generate the most accurate predictions. A temperature range 30 – 75 °C, and a gradient time range 3 – 12 minutes were evaluated using an initial to final %MeCN of 36 – 63% MeCN. It was found that there was no need to re-define the dwell volume (V_D) using an iterative process as excellent results were obtained with the calculated value of 517 µL using a slightly modified USP methodology for determining V_D [23].

Table 1 highlighted that the non-standard Equation 4 which described a curved relationship between log *k* and % organic generated more accurate retention time predictions (Δt_R <0.11%) than ~~that of~~ the standard Equation 3 (Δt_R <0.45%) for gradient time modelling.

In a similar manner, Table 2 highlighted that the non-standard Equation 6 which described a curved relationship between log retention factor (*k*) and 1/temperature generated more accurate retention time predictions (Δt_R<0.23%) than ~~that of~~ the standard Equations 5 (Δt_R<2.19%) for temperature modelling.

The LC simulator software utilizes empirical models to calculate peak widths (w_{base}) as shown in Equations 7, 8 and 9. Where α and β terms are fitted to minimize the residual for the retention time of the front ($t_{R\ front}$) and tail ($t_{R\ tail}$) of the peak.

$$t_{R\ tail} = (1 - \alpha)t_R \qquad \text{Equation 7}$$

$$t_{R\ front} = (1 + \beta)t_R \qquad \text{Equation 8}$$

$$w_{base} = t_{R\ front} - t_{R\ tail} \qquad \text{Equation 9}$$

It should be noted that Equations 1-9 describe isocratic separations, however, by employing numerical calculations where the gradients are divided into a large number of isocratic segments, these equations can be equally applied to gradient separations as described here.

From Tables 1 and 2 it can be seen that the commercially employed equations are able to model and predict the peak width to an acceptable degree with errors of <3% being observed with the models associated with Equations 4 and 6. As a result of the excellent retention time and acceptable peak width predictions excellent resolution predictions of <2% were obtainable when Equations 4 and 6 where employed, see Tables 1 and 2.

3.7.2 Gradient time *versus* temperature on the C18-AR at pH 6.8

As a result of the one-dimensional investigation (see section 3.7.1) the more complex Equations 6 and 4 were employed in the two-dimensional temperature and gradient time modelling. In order to model the non-linear relationships of temperature and gradient time on retention, described in Equations 6 and 4, sixteen input runs (i.e. 4 x 4) were used in order to generate high quality data.

From the two-dimensional model (see Figure 6), it is possible to iteratively change the V_D in order to minimize the predicted versus actual retention time errors for an experimental condition (gradient = 4.5 minutes and temperature = 30°C, often classed as a calibration run). However, the model using the determined V_D of 517 µL was shown to generate <0.08% error for retention time and was hence not changed.

The accuracy of the non-linear 4 x 4 retention model (total of 16 input experiments) was observed to be excellent. The prediction errors for t_R, peak width and resolution were <0.5 and <13.7% (most were below 5%), <7.8% respectively (see Table 3 and Figure 6) which is very good compared to the accepted accuracies of 2, 20 and 20% for t_R, peak width and resolution respectively [24, 25].

The resolution plot of gradient time versus temperature demonstrated that the methodology was robust (i.e. Rs >2) within the ranges of gradient time (3 to 12 minutes) and temperature (30 to 75°C), see Figure 6a.

A simplified 3 x 3 retention model (i.e. gradient times of 3, 6 and 9 minutes and temperatures of 30, 45 and 60°C, total of nine input experiments) which is sufficient to generate second order polynomial relationships generated results very similar to that seen in the more complex 4 x 4 model see Table 4.

It is interesting to note that if one employed the simple linear 2 x 2 retention modelling using the linear Equations 3 and 5 in a cut down four input data experiment (i.e. gradient times of 3 and 12 minutes and temperatures of 30 and 75°C), the retention time, peak width and resolution were <2.3 and <16.4%, <10.7% respectively which is still impressive given the substantially smaller number of experimental input runs that are required.

Conclusion

A detailed investigation into the retention behaviour and separation of the regioisomers of ~~the~~ methoxphenidine (i.e. 2-MXP, 3-MXP and 4-MXP isomers) has shown that, for this particular separation, the stationary phase chemistry is not a major selectivity parameter. At low pH, poor separation and retention of the MXP isomers was observed presumably due to mutual electrostatic repulsion of the adsorbed protonated analytes. In contrast, at intermediate pH, enhanced retention and separation of all MXP isomers was obtained, it appeared that there was a synergistic effect between the electrostatic and partitioning mechanisms. At high pH, the MXP isomers were retained by a predominantly hydrophobic mechanism due to their unionized form. It was observed that more complicated models were necessary to fully describe the retention of the MXP isomers due to the fact that multiple retention mechanisms were in operation. Using these non-linear models with 4 x 4 or 3 x 3 input runs, it was possible to predict with a high degree of certainly (<0.5%) the retention behaviour of the MXP isomers and then to optimize the gradient separation of the MXP isomers using a gradient and temperature design space. Prediction errors for peak width and resolution were in most cases lower than 5%. If one wishes to slightly sacrifice the prediction accuracy in favour of using a reduced number of experimental input runs, the linear models using a 2 x 2 model still generated retention time accuracy <2.3% yielding resolution accuracies of <11%.

Subsequently, from the 4 x 4 retention model, a rapid and highly sensitive LC-MS friendly method (i.e. $R_{s\ min} > 3$ within 2.5 minutes) was predicted and verified. The developed methodology should be highly suitable for the rapid, specific and sensitive detection and control of these novel illicit drugs within bulk forensic samples.

Conflict of interest

The authors have declared no conflict of interest.

Acknowledgements

The authors are grateful to the following: The Chromatographic Society for support through a summer studentship to B. Boateng; L. Steel and J. Field, Strathclyde Institute of Pharmacy and Biomedical Sciences (SIPBS) for performing the early column screening work and non-linear work respectively; Advanced Chemistry Development for providing the LC simulator and physical / chemical properties software and Advanced Chromatography Technologies for providing the columns used in this work.

518 References

519 [1] L. A. King, Legal Classification of Novel Psychoactive Substances: An International
520 Comparison, In Novel Psychoactive Substances, edited by P.I. Dargan, D.M. Wood,
521 Academic Press, Boston, (2013), Chapter 1, 3-27, ISBN 9780124158160,
522 http://dx.doi.org/10.1016/B978-0-12-415816-0.00001-8.

523 [2] S.W. Smith, F.M. Garlich, Availability and Supply of Novel Psychoactive Substances, In
524 Novel Psychoactive Substances, edited by P.I. Dargan, D.M. Wood, Academic Press,
525 Boston, (2013), Chapter 3, 55-77, ISBN 9780124158160,
526 http://dx.doi.org/10.1016/B978-0-12-415816-0.00003-1.

527 [3] M.C. Van Hout, E.Hearne, "Word of Mouse": Indigenous Harm Reduction and Online
528 Consumerism of the Synthetic Compound Methoxphenidine, J. Psychoactive Drugs,
529 47 (2015) 30-41.

530 [4] L.A. King, A.T. Kicman, A brief history of 'new psychoactive substances', Drug Test.
531 Anal., 3 (2011) 401–403.

532 [5] J. Wallach, P.V. Kavanagh, G. McLaughlin, N. Morris, J.D. Power, S.P. Elliot, M.S.
533 Mercier, D. Lodge, H. Morris, N.M. Dempster, S.D. Brandt, Preparation and
534 characterisation of the "research chemical" diphenidine, its pyrrolidine analogue,
535 and their 2,2-diphenylethyl isomers, Drug Test Anal. 7(5) (2015) 358-267.

536 [6] G. McLaughlin, N. Morris, P.V. Kavanagh, J.D. Power, J. O'Brien, B. Talbot, S.P. Elliott,
537 J. Wallach, K. Hoang, H. Morris, S.D. Brandt, Test purchase, synthesis, and
538 characterization of 2-methoxydiphenidine (MXP) and differentiation from its meta -
539 and para -substituted isomers. Drug Test Anal., 8 (2016) 98-109.
540 http://doi.org/10.1002/dta.1800

541 [7] H. Morris, J. Wallach, From PCP to MXE: a comprehensive review of the non-medical
542 use of dissociative drugs, Drug Test Anal. 6(7-8) (2016) 614-632.

543 [8] P. Reuter, B. Pardo, Can new psychoactive substances be regulated effectively? An
544 assessment of the British Psychoactive Substances Bill, Addiction 112 (1) (2017) 25-
545 31.

546 [9] A. Helander, O. Beck, M. Baeckberg, Intoxications by the dissociative new
547 psychoactive substance diphenidine and methoxphenidine, Clin Toxicol 53(5) (2015)
548 446-453.

549 [10] S.P. Elliot, S.D. Brandt, J. Wallach, H. Morris, P.V. Kavanagh, First reported fatalities
550 associated with the "research chemical" 2-methoxydiphenidine, J Anal Toxicol 39(4)
551 (2015) 287-293.

552

553

[11] P.M. Geyer, M.C. Hulme, J.P.B. Irving, P.D. Thompson, R.N. Ashton, R.J. Lee, L. Johnson, J. Marron, C.E. Banks and O.B. Sutcliffe, Guilty by Dissociation – Development of Gas Chromatography-Mass Spectrometry (GC-MS) and other rapid screening methods for the analysis of 13 diphenidine- derived New Psychoactive Substances (NPSs), Anal Bioanal Chem, 408 (29) (2016) 8467-8481.

[12] M.R. Euerby, M. Fever, J. Hulse, M. James, P. Petersson, C. Pipe, Maximization of Selectivity in Reverse Phase Liquid Chromatographic Method Development Strategies, LC●GC Europe, 29 (2016) 8 – 21.

[13] http://www.ace-hplc.com/technical-area/literature.aspx#2733. Accessed 3rd May 2016.

[14] M.R. Euerby, P. Petersson, Chromatographic classification and comparison of commercially available reversed-phase liquid chromatographic columns using principal component analysis, J. Chromatogr. A 994 (2003) 13-36.

[15] M.R. Euerby, P. Petersson, W. Campbell, W. Roe, Chromatographic classification and comparison of commercially available reversed-phase liquid chromatographic columns containing phenyl moieties using principal component analysis, J. Chromatogr. A 1154 (2007) 138-151.

[16] P. Jandera, M. Janderov, J. Churcek, Gradient elution in liquid chromatography: VIII. Selection of the optimal composition of the mobile phase in liquid chromatography under isocratic conditions, J Chromatogr. A 148 (1978) 79-97.

[17] Y. Baba, G. Kura, Computer-assisted retention prediction system for inorganic cyclic polyphosphates and its application to optimization of gradients in anion-exchange chromatography, J Chromatogr. A 550 (1991) 5-14.

[18] M.R. Euerby, J. Hulse, P. Petersson, A. Vazhentsev, K. Kassam, Retention Modelling in Hydrophilic Interaction Chromatography, Anal Bioanal Chem 40 (2015) 9135-9152.

[19] L.R. Snyder, J.W. Dolan, J.R. Gant, Gradient elution in high-performance liquid chromatography : I. Theoretical basis for reversed-phase systems, J Chromatogr. A 165 (1979) 3-30.

[20] P. Jandera, J. Churcek, L. Svoboda, Gradient elution in liquid chromatography: X. Retention characteristics in reversed-phase gradient elution chromatography, J Chromatogr. A 174 (1979) 35-50.

[21] P. Petersson, J. Munch, M.R. Euerby, A. Vazhentsev, M. McBrien, S.K. Bhal, K. Kassam, Adaption of Retention Models to Allow Optimisation of Peptide and Protein Separations. Chromatography Today 7 (2007) 15-18.

[22] T. Galaon, V. David, Deviation from van't Hoff dependence in RP-LC induced by tautomeric interconversion observed for four compounds, J Sep Sci 34 (2011) 1423-1428.

[23] Chromatographic system suitability tests signal to noise USP 37 <621> https://hmc.usp.org/sites/default/files/documents/HMC/GCs-Pdfs/c621.pdf. Accessed 19th December 2016

[24] R.G. Wolcott, J.W. Dolan, L.R. Snyder, Computer simulation for the convenient optimization of isocratic reversed-phase liquid chromatographic separations by varying temperature and mobile phase strength, J Chromatogr. A 869 (2000) 3-25,

[25] L.R. Snyder, J.W. Dolan, High-Performance Gradient Elution: The Practical Application of the Linear-Solvent-Strength Model, Hoboken, NJ: Wiley, (2007) pp. 399.

603 Highlights

604 • Retention / separation of MXP regioisomers is controlled by electrostatic /
605 hydrophobic mechanisms
606 • Non-linear models were generated to describe the effect of % organic and
607 temperature on retention
608 • Two-dimensional (gradient time versus temperature) modelling was highly accurate
609 • Rapid separation of MXP regioisomers was achieved by retention modelling and
610 optimization
611 • A rapid / highly sensitive LC-MS method ($R_{s\ min}$ > 3 within 2.5 minutes) was predicted
612 and verified

613

614 Graphical highlight

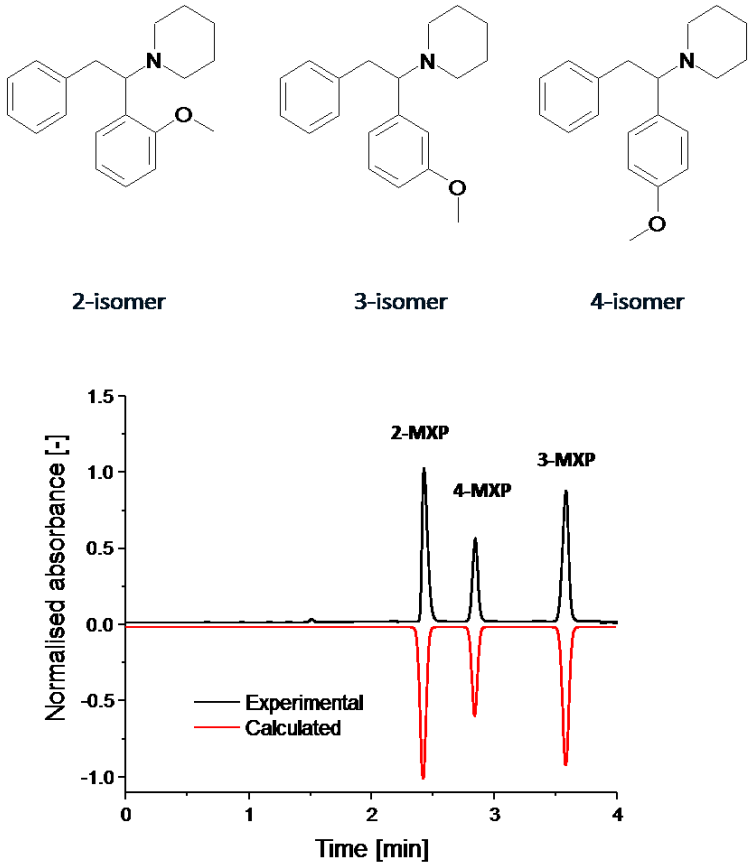

615

616

Figure 1. Structure of the diphenidine (1) and methoxydiphenidine regioisomers (2, 2-MXP; 3, 3-MXP and 4, 4-MXP).

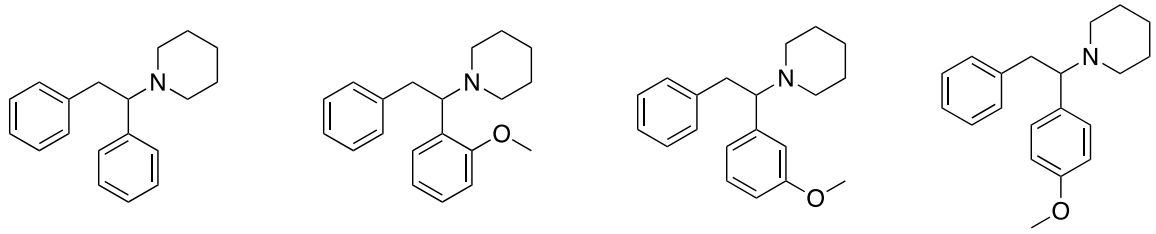

Diphenidine (**1**)

2-Methoxphenidine (**2**, 2-MXP)

3-Methoxphenidine (**3**, 3-MXP)

4-Methoxphenidine (**4**, 4-MXP)

Figure 2 Separation of the MXP isomers (2-, 3- and 4-isomers) on an ACE UltraCore SuperC18 2.5 µm 50 x 4.6 mm column, 50 °C, 1 mL min^{-1}, Agilent 1290 Infinity Quaternary UHPLC, mobile phase of MeCN : water (54:46 v/v) containing a) 10 mM ammonium formate pH 3, b) 10 mM ammonium acetate (unadjusted pH of 6.8) and c) 18 mM ammonia (unadjusted pH of 10.7). MXP isomer assignment as shown in the chromatograms.

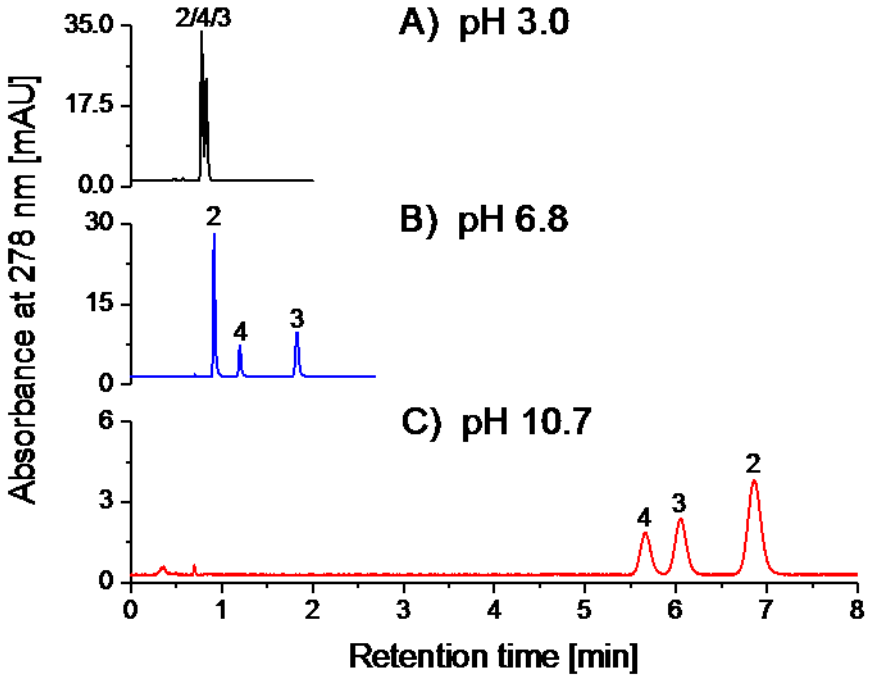

Figure 3. Effect of buffer concentration on the retention on the regioisomers at pH 6.8 using an ACE C18-AR, 3 µm, 50 x 4.6 mm column, ammonium acetate (pH 6.8) in MeCN/water (54:46 v/v), 30 °C, 1 mL min^{-1}, Agilent 1290 Infinity quaternary UHPLC.

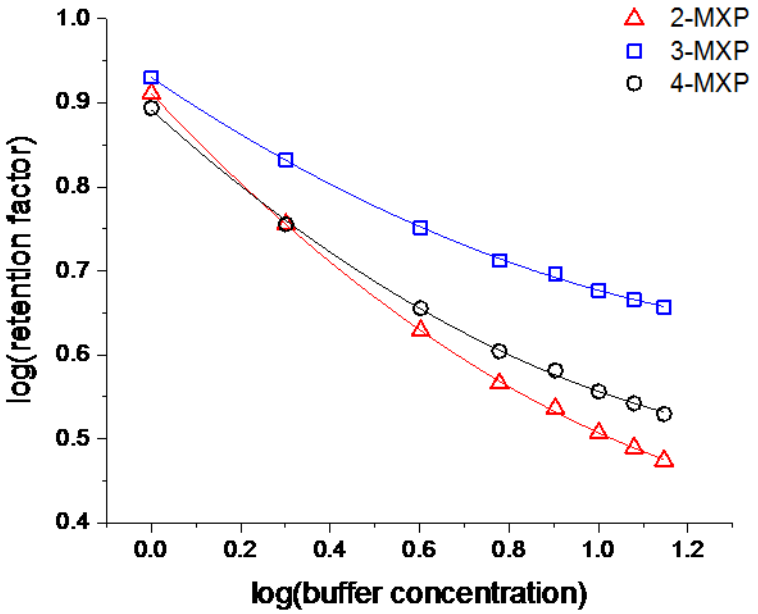

644 Figure 4. The effect of the proportion of MeCN, on the retention of the MXP
645 isomers performed on an ACE SuperC18 3 µm 50 x 4.6 mm column, 1
646 mL min^{-1}, 60 °C, Agilent 1290 Infinity binary UHPLC. Mobile phase A
647 buffer in water, mobile phase B buffer in MeCN/water (9:1 v/v).

648

649 4a) buffer 10 mM ammonium formate (pH 3.0).

650 4b) buffer 10 mM ammonium acetate (pH 6.8 unadjusted).

651 4c) buffer 18.6 mM ammonia (pH 10.7).

652

653

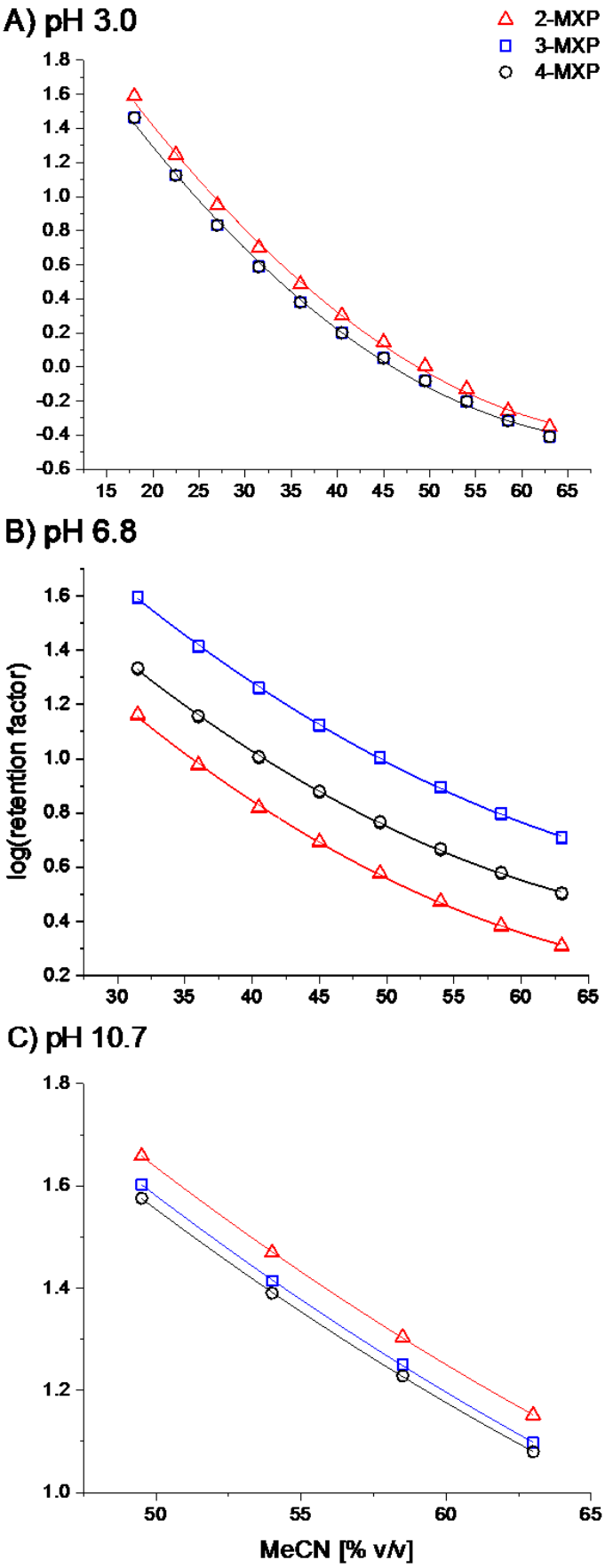
A) pH 3.0
2-MXP
3-MXP
4-MXP
B) pH 6.8
log(retention factor)
C) pH 10.7
MeCN [% v/v]

654

Figure 5. The effect of 1/temperature (°K) on the log of the retention factor of the MXP isomers performed on an ACE C18-AR 3 µm 50 x 4.6 mm column using 10 mM ammonium acetate (pH 6.8 unadjusted) in MeCN/water 54:46 v/v, 1 mL min^{-1} using the Shimadzu Nexera X2 UHPLC.

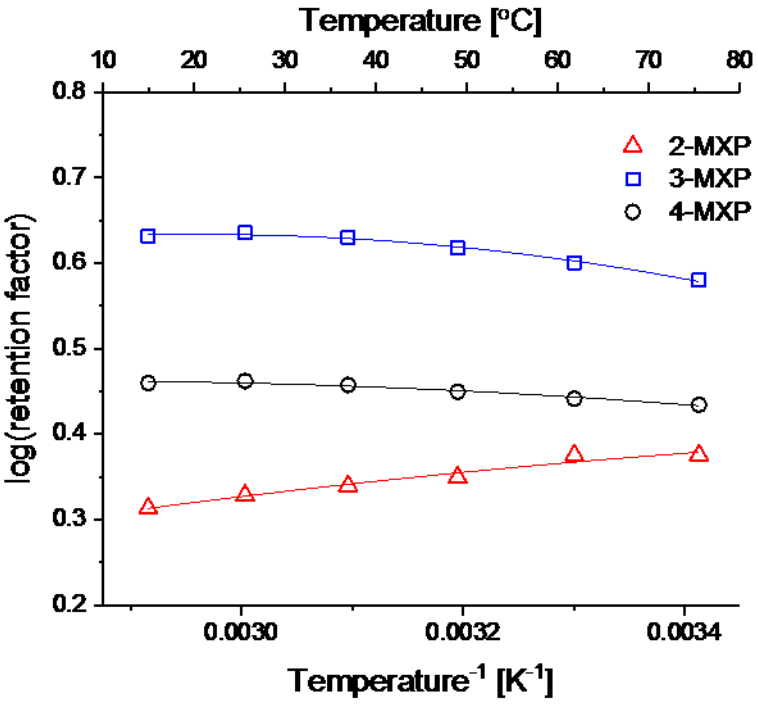

Figure 6. a) Two-dimensional retention model (gradient time versus temperature) for the ACE C18-AR, 3 µm, 50 x 4.6 mm column, 1 mL min^{-1}, mobile phase A) 10 mM ammonium acetate (pH 6.8 unadjusted) in water and B) 10 mM ammonium acetate (pH 6.8 unadjusted) in MeCN/water (9:1 v/v), gradient 40 to 70%B, Nexera X2 UHPLC with a V_D and V_m of 517 and 458 µL respectively.

b) Experimental and predicted chromatograms performed with a gradient and temperature of 4.5 min and 60 °C.

Figure 6a

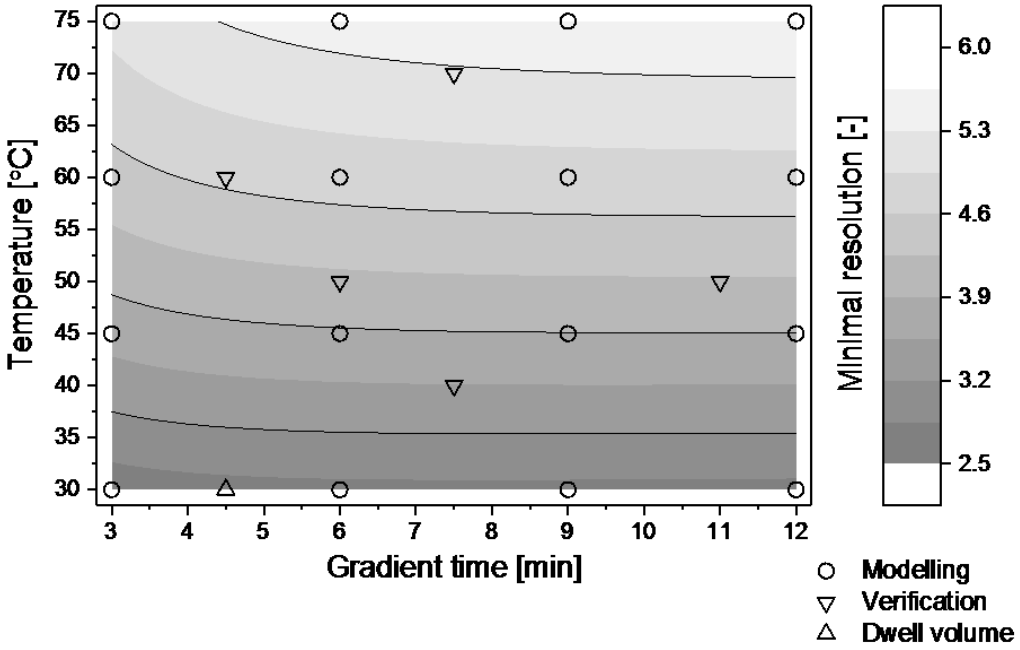

674 Figures 6b

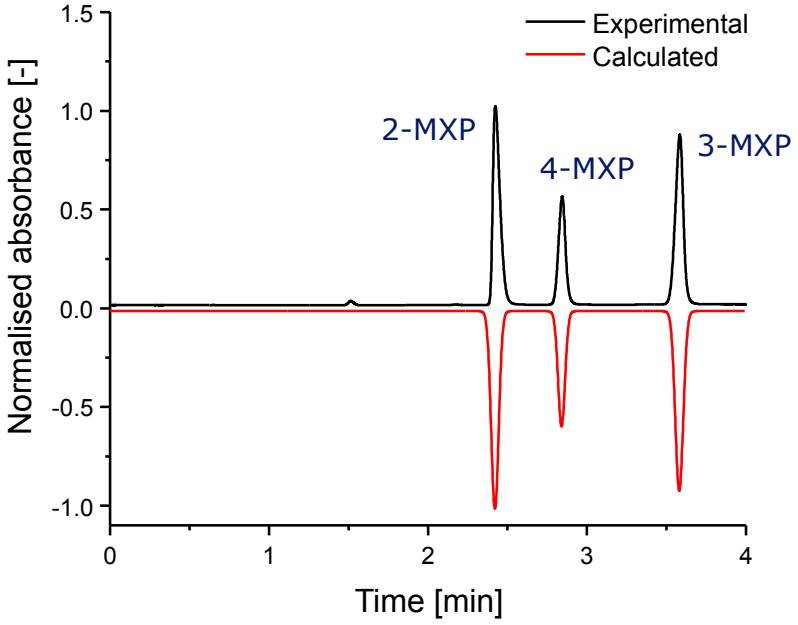

675

676

677

678 Table 1. Prediction errors for gradient time models using Equations 3 (gradient inputs of 3
679 and 12 min) and 4 (gradient inputs of 3, 6, 9 and 12 min) as assessed by an interpolation of
680 the retention at a gradient time of 4.5 minutes using a temperature of 30°C, where %Δ
681 retention time (t_R) = (predicted t_R – actual t_R)/ actual t_R, %Δ peak width at 4 x standard
682 deviation (4σ) = (predicted peak width at 4σ – actual peak width at 4σ)/ actual peak width at
683 4σ, %Δ R_s at 4σ = (predicted resolution (R_s) at 4σ – actual R_s at 4σ)/ actual R_s at 4σ. V_D and the
684 column void volume (V_m) = 517 and 458 µL respectively.

685

Equation 3	Predicted			Actual									
Peak Name	t_R (min)	Width (min)	R_s (USP)	t_R (min)	Width (min)	R_s (USP)	Δ tR (min)	%Δ t_R	Δ width (min)	%Δ width	Δ R_s (USP)	%Δ R_s (USP)	Model used
2-MXP	2.486	0.108		2.477	0.109		0.009	0.36	-0.001	-0.65			a = 4.9666, b = -7.8663e-2, c = 0.0000
4-MXP	2.729	0.088	2.48	2.72	0.087	2.49	0.009	0.33	0.001	1.59	-0.01	-0.34	a = 4.8601, b = -7.2282e-2, c = 0.0000
3-MXP	3.378	0.096	7.05	3.363	0.099	6.95	0.015	0.45	-0.003	-2.55	0.11	1.56	a = 5.0037, b = -6.6316e-2, c = 0.0000

Equation 4	Predicted			Actual									
Peak Name	t_R (min)	Width (min)	R_s (USP)	t_R (min)	Width (min)	R_s (USP)	Δ tR (min)	%Δ t_R	Δ width (min)	%Δ width	Δ R_s (USP)	%Δ R_s (USP)	Model used
2-MXP	2.475	0.110		2.477	0.109		-0.002	-0.08	0.001	1.19			a = 7.7101, b = -1.9844e-1, c = 1.2937e-3
4-MXP	2.717	0.088	2.44	2.720	0.087	2.49	-0.003	-0.11	0.001	1.59	-0.04	-1.75	a = 7.0448, b = -1.6585e-1, c = 9.8928e-4
3-MXP	3.361	0.100	6.85	3.363	0.099	6.95	-0.002	-0.06	0.001	1.51	-0.10	-1.37	a = 6.7427, b = -1.3715e-1, c = 7.0815e-4

686

687

688

689 Table 2. Accuracy of the temperature models using Equations 5 (temperature inputs of 30
690 and 70°C) and 6 (temperature inputs of 30, 45, 60 and 70°C) as assessed by an interpolation
691 of the retention at 50°C using a gradient time of 6 minutes where %Δ t_R = (predicted t_R –
692 actual t_R)/ actual t_R, %Δ peak width at 4σ = (predicted peak width at 4σ – actual peak width
693 at 4σ)/ actual peak width at 4σ, %Δ R_s at 4σ = (predicted R_s at 4σ – actual R_s at 4σ)/ actual R_s
694 at 4σ. V_D and V_m = 517 and 458 µL respectively.

695

Equation 5	Predicted			Actual									
Peak	t_R (min)	Width (min)	R_s (USP)	t_R (min)	Width (min)	R_s (USP)	Δ tR (min)	%Δ t_R	Δ width (min)	%Δ width	Δ R_s (USP)	%Δ R_s (USP)	Model
2-MXP	2.547	0.106		2.574	0.100		-0.027	-1.05	0.006	5.78			a = 1.1179, b = 1.2912e+2
4-MXP	2.947	0.097	3.94	2.988	0.093	4.28	-0.041	-1.37	0.004	3.83	-0.34	-7.84	a = 2.1439, b = -1.4570e+2
3-MXP	3.747	0.112	7.66	3.831	0.109	8.34	-0.084	-2.19	0.003	3.03	-0.69	-8.22	a = 2.5724, b = -1.9410e+2

Equation 6	Predicted			Actual									
Peak	t_R (min)	Width (min)	R_s (USP)	t_R (min)	Width (min)	R_s (USP)	Δ tR (min)	%Δ t_R	Δ width (min)	%Δ width	Δ R_s (USP)	%Δ R_s (USP)	Model
2-MXP	2.568	0.103		2.574	0.100		-0.006	-0.23	0.003	2.78			a = -9.8483e-1, b = 1.4981e+3, c = -2.2174e+5
4-MXP	2.985	0.095	4.21	2.988	0.093	4.28	-0.003	-0.10	0.002	1.69	-0.06	-1.50	a = -1.0249, b = 1.9168e+3, c = -3.3403e+5
3-MXP	3.829	0.111	8.19	3.831	0.109	8.34	-0.002	-0.05	0.002	2.11	-0.15	-1.77	a = -2.5816, b = 3.1609e+3, c = -5.4338e+5

696

697

Table 3. Predicted, actual and accuracy of retention time, peak width and resolution from the two-dimensional models (see Figure 6) using equation 4 (t_G inputs of 3, 6, 9 and 12 min) and equation 6 (temperature inputs of 30, 45, 60 and 70°C) as assessed by five interpolation conditions within the design space, where %Δ t_R = (predicted t_R – actual t_R)/ actual t_R, %Δ peak width at 4σ = (predicted peak width at 4σ – actual peak width at 4σ)/ actual peak width at 4σ, %Δ R_s at 4σ = (predicted R_s at 4σ – actual R_s at 4σ)/ actual R_s at 4σ. V_D and V_m = 517 and 458 µL respectively.

	Temperature (°C)	t_G (min)	Predicted			Actual								
Peak	70	7.5	**t_R (min)**	**Width (min)**	**R_s (USP)**	**t_R (min)**	**Width (min)**	**R_s (USP)**	**Δ tR (min)**	**%Δ t_R**	**Δ width (min)**	**%Δ width**	**Δ R_s (USP)**	**%Δ R_s (USP)**
2-MXP			2.585	0.111		2.576	0.098		0.010	0.37	0.013	13.27		
4-MXP			3.151	0.105	5.24	3.145	0.103	5.67	0.006	0.19	0.002	1.94	-0.43	-7.52
3-MXP			4.121	0.126	8.40	4.117	0.124	8.56	0.005	0.11	0.002	1.61	-0.16	-1.88
Peak	50	6	**t_R (min)**	**Width (min)**	**R_s (USP)**	**t_R (min)**	**Width (min)**	**R_s (USP)**	**Δ tR (min)**	**%Δ t_R**	**Δ width (min)**	**%Δ width**	**Δ R_s (USP)**	**%Δ R_s (USP)**
2-MXP			2.566	0.104		2.574	0.100		-0.008	-0.31	0.004	4.00		
4-MXP			2.982	0.095	4.18	2.988	0.093	4.30	-0.006	-0.20	0.002	2.15	-0.12	-2.77
3-MXP			3.827	0.113	8.13	3.831	0.109	8.30	-0.004	-0.10	0.004	3.67	-0.18	-2.11
			Predicted			**Actual**								
Peak	50	11	**t_R (min)**	**Width (min)**	**R_s (USP)**	**t_R (min)**	**Width (min)**	**R_s (USP)**	**Δ tR (min)**	**%Δ t_R**	**Δ width (min)**	**%Δ width**	**Δ R_s (USP)**	**%Δ R_s (USP)**
2-MXP			2.793	0.124		2.792	0.123		0.001	0.04	0.002	1.22		
4-MXP			3.303	0.117	4.23	3.302	0.115	4.29	0.002	0.05	0.002	1.74	-0.06	-1.36
3-MXP			4.415	0.146	8.46	4.411	0.144	8.58	0.004	0.09	0.003	1.74	-0.13	-1.49
			Predicted			**Actual**								
Peak	60	4.5	**t_R (min)**	**Width (min)**	**R_s (USP)**	**t_R (min)**	**Width (min)**	**R_s (USP)**	**Δ tR (min)**	**%Δ t_R**	**Δ width (min)**	**%Δ width**	**Δ R_s (USP)**	**%Δ R_s (USP)**
2-MXP			2.420	0.094		2.423	0.085		-0.003	-0.12	0.009	10.59		
4-MXP			2.840	0.086	4.67	2.843	0.083	5.00	-0.003	-0.11	0.003	3.61	-0.33	-6.67
3-MXP			3.580	0.099	8.00	3.584	0.095	8.32	-0.003	-0.10	0.004	4.21	-0.32	-3.85
			Predicted			**Actual**								
Peak	40	7.5	**t_R (min)**	**Width (min)**	**R_s (USP)**	**t_R (min)**	**Width (min)**	**R_s (USP)**	**Δ tR (min)**	**%Δ t_R**	**Δ width (min)**	**%Δ width**	**Δ R_s (USP)**	**%Δ R_s (USP)**
2-MXP			2.680	0.112		2.672	0.117		0.009	0.32	-0.005	-4.27		
4-MXP			3.059	0.102	3.54	3.047	0.102	3.43	0.013	0.41	0.000	0.49	0.11	3.19
3-MXP			3.955	0.122	8.00	3.940	0.122	7.99	0.016	0.39	0.000	0.00	0.01	0.11

Table 4. Predicted, actual and accuracy of retention time, peak width and resolution from the two-dimensional models using equation 4 (t_G inputs of 3, 6 and 9 min) and equation 6 (temperature inputs of 30, 45 and 60°C) as assessed by three interpolation conditions within the design space, where %Δ t_R = (predicted t_R – actual t_R)/ actual t_R, %Δ peak width at 4σ = (predicted peak width at 4σ – actual peak width at 4σ)/ actual peak width at 4σ, %Δ R_s at 4σ = (predicted R_s at 4σ – actual R_s at 4σ)/ actual R_s at 4σ. V_D and V_m = 517 and 458 µL respectively.

	Temperature (°C)	t_G (min)	Predicted			Actual								
Peak	50	6	**t_R (min)**	**Width (min)**	**R_s (USP)**	**t_R (min)**	**Width (min)**	**R_s (USP)**	**Δ tR (min)**	**%Δ t_R**	**Δ width (min)**	**%Δ width**	**Δ R_s (USP)**	**%Δ R_s (USP)**
2-MXP			2.567	0.107		2.574	0.100		-0.008	-0.31	0.004	4.00		
4-MXP			2.984	0.096	4.11	2.988	0.093	4.30	-0.006	-0.20	0.002	2.15	-0.19	-4.46
3-MXP			3.828	0.113	8.08	3.831	0.109	8.30	-0.004	-0.10	0.004	3.67	-0.22	-2.69
			Predicted			**Actual**								
Peak	60	4.5	**t_R (min)**	**Width (min)**	**R_s (USP)**	**t_R (min)**	**Width (min)**	**R_s (USP)**	**Δ tR (min)**	**%Δ t_R**	**Δ width (min)**	**%Δ width**	**Δ R_s (USP)**	**%Δ R_s (USP)**
2-MXP			2.422	0.096		2.423	0.085		-0.003	-0.12	0.009	10.59		
4-MXP			2.841	0.086	4.60	2.843	0.083	5.00	-0.003	-0.11	0.003	3.61	-0.40	-7.91
3-MXP			3.581	0.099	8.00	3.584	0.095	8.32	-0.003	-0.10	0.004	4.21	-0.32	-3.85
			Predicted			**Actual**								
Peak	40	7.5	**t_R (min)**	**Width (min)**	**R_s (USP)**	**t_R (min)**	**Width (min)**	**R_s (USP)**	**Δ tR (min)**	**%Δ t_R**	**Δ width (min)**	**%Δ width**	**Δ R_s (USP)**	**%Δ R_s (USP)**
2-MXP			2.679	0.115		2.672	0.117		0.009	0.32	-0.005	-4.27		
4-MXP			3.059	0.102	3.50	3.047	0.102	3.43	0.013	0.41	0.000	0.49	0.07	2.03
3-MXP			3.955	0.123	7.96	3.940	0.122	7.99	0.016	0.39	0.000	0.00	-0.03	-0.33